fishes

MDPI

Article

Gene Expression and Epigenetic Modification of Aromatase during Sex Reversal and Gonadal Development in Blotched Snakehead (*Channa maculata*)

Sujing Huang [1,2], Yuxia Wu [1,2], Kunci Chen [1,2], Xiaotian Zhang [1,2], Jian Zhao [1,2], Qing Luo [1], Haiyang Liu [1], Fang Wang [1], Kaibin Li [1,2], Shuzhan Fei [1], Xincheng Zhang [1] and Mi Ou [1,3,*]

[1] Key Laboratory of Tropical and Subtropical Fishery Resources Application and Cultivation, Ministry of Agriculture and Rural Affairs, Pearl River Fisheries Research Institute, Chinese Academy of Fishery Sciences, Guangzhou 510380, China
[2] College of Fisheries and Life Science, Shanghai Ocean University, Shanghai 201306, China
[3] School of Life Sciences, Hunan University of Science and Technology, Xiangtan 411201, China
* Correspondence: om1990@prfri.ac.cn; Tel.: +86-020-816165099

Abstract: The *cyp19a1* gene codes aromatase that converts androgen to estrogen, which plays a central role in early female differentiation and ovarian development in teleosts. For the blotched snakehead (*Channa maculata*), an important aquaculture fish that is susceptible to hormone-induced sex reversal, two aromatase genes were characterized in the present study, *cyp19a1a* and *cyp19a1b*. We analyzed gene expression and the epigenetic state of *cyp19a1a* and *cyp19a1b* in different adult tissues: the gonad and brain from normal XX females (XX-F), normal XY males (XY-M), sex-reversal females (XY-F) induced by estrogen, and YY super-males (YY-M), and gonads at different development stages. *Cyp19a1a* exhibited strong female-biased expression patterns in the ovary, and *cyp19a1b* dominantly expressed in the brain with no sex bias. *Cyp19a1a*'s expression pattern in the XY-F ovary was similar to that in the XX-F ovary, with a relatively high expression level, which was far higher than that in XY-M and YY-M testis. Meanwhile, CpG methylation levels of *cyp19a1a* promoter were lower in XX-F and XY-F ovaries compared with XY-M and YY-M testis. A significantly negative correlation between the CpG methylation levels and *cyp19a1a* expression was elucidated in XX-F, XY-M, XY-F, and YY-M gonads. Furthermore, the strong female-biased *cyp19a1a* expression was closely related to ovarian differentiation and maturation, and the overall methylation levels of *cyp19a1a* promoter were inversely correlated with *cyp19a1a* expression. There were no detectable sexually dimorphic differences in *cyp19a1b* expression and CpG methylation levels of *cyp19a1b* promoter in the brain and gonad between sexes in *C. maculata*, thus the function of *cyp19a1b* in *C. maculata* needs further research. Our research illustrates that cyp19a1a is closely related to estrogen production, ovary differentiation/maintenance, and sex reversal, and epigenetic modification plays a crucial part in maintaining the sexual dimorphic expression of *cyp19a1a*, ovarian differentiation and oogenesis in *C. maculata*.

Keywords: aromatase; sex reversal; gene expression; CpG methylation; *Channa maculata*

Citation: Huang, S.; Wu, Y.; Chen, K.; Zhang, X.; Zhao, J.; Luo, Q.; Liu, H.; Wang, F.; Li, K.; Fei, S.; et al. Gene Expression and Epigenetic Modification of Aromatase during Sex Reversal and Gonadal Development in Blotched Snakehead (*Channa maculata*). *Fishes* **2023**, *8*, 129. https://doi.org/10.3390/fishes8030129

Academic Editors: Dong-Neng Jiang, Hong-Wei Yan and Li-Min Wu

Received: 7 December 2022
Revised: 21 February 2023
Accepted: 21 February 2023
Published: 24 February 2023

1. Introduction

Sex is one of the important propositions in biological science, and also a hotspot and difficulty in aquaculture [1]. Since the discovery of the *Sry* gene in mammals [2], important progress has been made in the mechanism of sex determination and differentiation [3,4], which exhibits diversity across different animal species. As primitive vertebrates, the sex determination and gonadal differentiation of fish is the comprehensive result of the interaction between genetic (sex-determining regulatory network) and environmental (exogenous hormone, temperature, pH, and so on) factors [5,6]. Despite diversity in sex-determination

systems and master sex-determining genes, the downstream genetic network of sex differentiation and the basic pattern of gonadal development are relatively conservative [7]. *Dmrt1* (*doublesex- and mab-3-related transcription factor 1*) and *gsdf* (*gonadal soma-derived factor*) are usually contained in the male pathway, while *foxl2* (*forkhead transcription factor 2*) and *cyp19a1* (*cytochrome P450, family 19, subfamily A*) are usually contained in the female pathway, and these genes consistently show sexual dimorphism during gonadal differentiation and development [8–11].

The *cyp19a1* gene codes for an aromatase that is a sex steroid hormone, which is responsible for the conversion of androgen to estrogen, and thus is highly relevant to sex reversal [12,13]. Aromatase in most tetrapods is encoded by a single *cyp19a1* gene [14–16], but due to the teleost-specific third round of whole-genome duplication (TWGD, 3R), two aromatase genes are characterized in substantial teleosts, namely, ovarian aromatase (*cyp19a1a*) and brain aromatase (*cyp19a1b*) [17]. These two aromatase genes have evolved into largely different roles. *Cyp19a1a* has a female-biased expression pattern in teleost, which is inferred to be intimately related to estrogen production and ovary differentiation/maintenance [10,12]. *Cyp19a1b* is mainly expressed in the brain but also in other tissues, which plays a role in multifaceted aspects such as sexual behavior, neural development, etc. [18,19].

During the undifferentiated gonad stage, fish sex can be reversed by the induction of exogenous estrogen or the interruption of endogenous estrogen synthesis with aromatase inhibitor, so as to achieve sex control and obtain a monosex population with higher aquaculture value [4,20]. The conserved *cyp19a1* gene is usually involved in the process of sex reversal. Decreased *cyp19a1a* expression and estrogen levels are considered potential triggers of female-to-male sex reversal; conversely, increased *cyp19a1a* expression and estrogen levels are associated with the male-to-female sex reversal [6]. Epigenetic modification has been found to contribute to the regulation of *cyp19a1a* expression in the switching of sex pathways in sex-changing or environment-sensitive fish [21,22]. In rice field eel (*Monopterus albus*), increased DNA methylation levels of *cyp19a1a* promoter were found in the gonads during female-to-male sex reversal. Significantly, the treatment of DNA methylation inhibitor could reverse the natural female-to-male sex reversal [23]. In orange-spotted grouper (*Epinephelus coioides*), increased methylation levels of *cyp19a1a* promoter were associated with maleness during female-to-male sex reversal [24]. In black porgy (*Acanthopagrus schlegelii*), male-to-female sex reversal occurred after the testis was dislodged from the digonic gonad, and the methylation levels of *cyp19a1a* promoter were significantly reduced in the ovary [25]. Furthermore, high-temperature treatment resulted in the significantly increased methylation of *cyp19a1a* promoter and led to suppressed *cyp19a1a* expression and testicular development in European sea bass (*Dicentrarchus labrax*) [26], half-smooth tongue sole (*Cynoglossus semilaevis*) [27], Japanese flounder (*Paralichthys olivaceus*) [28], and Nile tilapia (*Oreochromis niloticus*) [29]. Therefore, *cyp19a1a* is a candidate gene for exploring the relationship between DNA methylation and sex maintenance.

Blotched snakehead (*Channa maculata*) is an important aquaculture fish, which is mainly distributed in southern China, the Philippines, and Vietnam. In China, the annual production of snakehead has increased yearly, and reached 548,481 tons in 2021 [30]. Significant sexual dimorphisms commonly exist in the growth speed and body size of snakehead, males are 1.5–2.0 times larger than females, and the large and uniform individuals garner a high price in snakehead trading; thus, an all-male population with higher commercial values is preferred in aquaculture [31]. In blotched snakehead, male-to-female sex reversal could be induced by the exogenous estrogen administration, thus sex reversal females (XY-F) were obtained, and XY all-male (XY-M) populations were produced by mating YY super-males (YY-M) with normal XX females (XX-F) [32]. However, the sex reversal rate was not very high, and the optimization of estrogen treatment is the premise for improving the productivity of all-male populations. According to the transcriptome analysis on four types of gonads from XY-F, XX-F, XY-M, and YY-M blotched snakehead, two *cyp19a1* genes (ovary-specific *cyp19a1a* and brain-specific *cyp19a1b*) were found in *C. maculata*, and

cyp19a1a expression showed obvious sexual dimorphism in gonads [31]. It suggested that cyp19a1 may play an important role in ovarian development and maintenance in snakehead; therefore, functional studies on cyp19a1 may provide theoretical support for the optimization of estrogen treatment. In this study, the sequences and gene structures of *cyp19a1a* and *cyp19a1b* were characterized, and gene expression analyses in different adult tissues and in gonads during developmental stage were performed. DNA methylation analyses in both adult gonad and brain tissue were investigated in XX-F, XY-F, XY-M, and YY-M blotched snakehead. Furthermore, DNA methylation analyses were also conducted on gonads at different developmental stages between XX-F and XY-M individuals. The study is aimed at clarifying the structure and expression pattern of *cyp19a1* gene in *C. maculata* and at exploring whether epigenetic modification can regulate *cyp19a1* expression in the sex reversal and gonadal development in blotched snakehead.

2. Materials and Methods

2.1. Animal and Sample Collection

Experimental fish were cultured in the fish laboratory of the Model Animal Research Center, Pearl River Fisheries Research Institute (Guangzhou City, Guangdong Province, China). Various tissues including gills, middle kidney, liver, heart, intestines, gonads, muscle, spleen, head kidney, and brain were collected from adult XX-F (n = 3, body weight, 603.2 ± 29.8 g; body length: 32.1 ± 1.1 cm) and XY-M (n = 3, body weight, 776.0 ± 43.1 g; body length: 35.3 ± 1.3 cm) individuals. These tissue samples were used for gene cloning, expression, and DNA methylation analyses. In addition, XY-F (n = 3, body weight, 579.3 ± 28.7 g; body length: 30.9 ± 1.0 cm) and YY-M individuals (n = 3, body weight, 774.5 ± 38.7 g; body length: 35.4 ± 1.2 cm) were differentiated by genetic sex identification and histological section as we previously reported [33]; gonads and brain were individually dissected for expression and DNA methylation analyses. Furthermore, the gonads from XX-F and XY-M individuals (n = 3) at different developmental stages (30, 60, 90, 120, 150, and 180 days post-fertilization (dpf)) were obtained for the expression and DNA methylation analyses, and the genetic sex was identified as mentioned above. All tissue samples were immediately immersed in liquid nitrogen and stored at −80 °C.

2.2. Full-Length cDNA Cloning and Sequence Analysis

Two aromatase genes were identified in the blotched snakehead genome (SRA Accession No. PRJNA730430) [34], ovarian aromatase *cyp19a1a*, and brain aromatase *cyp19a1b*, and the predicted cDNA sequences of *cyp19a1a* and *cyp19a1b* were obtained. RNA isolation, cDNA synthesis, and gene cloning and sequencing were performed as described previously [33]. In brief, Cyp19a1a-F1/R1 and Cyp19a1b-F1/R1 primer pairs were used to verify the predicted cDNA sequences. Subsequently, the 5′ and 3′ untranslated regions (UTRs) were gained by specific and adaptor primers using 5′-RACE and 3′-RACE Ready cDNA as templates, respectively. Then, the full-length cDNA sequences within the 5′ and 3′ UTRs were amplified by Cyp19a1a-F2/R2 and Cyp19a1b-F2/R2 primer pairs. Lastly, positive colonies including the target fragment were selected and sequenced by the commercial company (Sangon Biotech, Shanghai, China). The primers are shown in Table 1. The sequence analyses of nucleotide and amino acid were conducted as previously described [33].

Plentiful aromatase protein sequences from 26 species were selected from NCBI (https://www.ncbi.nlm.nih.gov/, accessed on 7 November 2022) to construct the phylogenetic tree for the study of sequence similarities and molecular evolution, including *C. maculata*, *Larimichthys crocea*, *Mus musculus*, *Perca flavescens*, *Oryzias latipes*, *Bos taurus*, *O. niloticus*, *M. albus*, *Takifugu rubripes*, *Salmo salar*, *Gallus gallus*, *Ictalurus punctatus*, *Strigops habroptila*, *Heteropneustes fossilis*, *Danio rerio*, *Xenopus laevis*, *Numida meleagris*, *Carassius auratus*, *Cyprinus carpio*, *Xenopus tropicalis*, *Acipenser baerii*, *Lepisosteus oculatus*, *Callorhinchus milii*, *Carcharodon carcharias*, *Hypanus sabinus*, and *Homo sapiens*. The phylogenetic tree was analyzed using Mega 6.0 with the neighbor-joining (NJ) algorithms, and bootstrap values

were calculated with 1000 replications. The alignments among these aromatase protein sequences were conducted using ClustalX2.

Table 1. Primers for full-length cDNA cloning, qRT-PCR, BSP analysis, and knockout detection.

Primer Name	Sequence (5′–3′)	Application
Cyp19a1a-F1	GCACTGCCAGCAACTACTAC	partial sequence obtaining
Cyp19a1a-R1	AATGGCTGGAAGTAACGAC	
Cyp19a1b-F1	AGTCACTGCGATTCTGCTTCT	
Cyp19a1b-R1	CGACAGGTTGTTGGTCTGC	
Cyp19a1a-5′F-out	GCAAGTGTATTGTCCA	5′-Race PCR amplification
Cyp19a1a-5′F-in	GGGTCTCCTCTCCATTGA	
Cyp19a1b-5′F-out	GCTTGCTGTTCCAATC	
Cyp19a1b-5′F-in	AAGTCCTGCTAGGAAACG	
Cyp19a1a-3′F-out	CCCTGTCTGATGACATCATAGATGGCTAC	3′-Race PCR amplification
Cyp19a1a-3′F-in	TCTCAAACAAAATGAATTCAGTCTGGAG	
Cyp19a1b-3′F-out	CCAATATCATTCTCAACATTGGTCTCATGC	
Cyp19a1b-3′F-in	GTGATGATGAAGGCCATCTTGGTCACTC	
Cyp19a1a-F2	ATTGTGTCAAGTCTCCCTC	ORF qualifying
Cyp19a1a-R2	TCTCACTATGTGGACTCG	
Cyp19a1b-F2	TGTACTGGTGAGAGACACTT	
Cyp19a1b-R2	AGGGATGCTGTTACACATC	
Cyp19a1a-BSP-F1	TTTTTAAGAGTGTAGGTATAAATT	DNA methylation analysis
Cyp19a1a-BSP-R1	TCCTACCTAAAACATTATTCTTA	
Cyp19a1b-BSP-F1	TGTGGTTTTAACGAGTAATGTT	
Cyp19a1b-BSP-R1	TTACGAAAATAAATAACAAAAAACTA	
Cyp19a1a-qF	CCTCGTCGTTACTTCCAGCC	qRT-PCR amplification
Cyp19a1a-qR	TCAAACCCTTATGGAGGCAAA	
Cyp19a1b-qF	GTGCCGCTAAACGAGAAAGA	
Cyp19a1b-qR	GGTTCTGGGCAAGGATGAG	
β-actin-qF	AGCAAGCAGGAGTATGATGA	
β-actin-qR	AGAACGCCAGGGAGTTTTAT	
EF1α-qF	GGGACACCCACAATAACATCC	
EF1α-qR	CCAGGCATACTTGAAGGAGC	

2.3. Expression Analysis Using qRT-PCR

qRT-PCR was performed to determine the mRNA expression levels of *cyp19a1a* and *cyp19a1b* in different adult tissues and during gonadal development in *C. maculata*. The first strand cDNAs used for qRT-PCR were synthetized separately from different samples using ReverTra Ace® qPCR RT Master Mix with gDNA Remover (Toyobo, Japan) following the manufacturer's protocol. *β-actin* and *EF1α* were utilized as internal controls to normalize the gene expression level [35]. Specific primers (Table 1) were designed for qRT-PCR. Expression analysis of *cyp19a1a*, *cyp19a1b*, *β-actin*, and *EF1α* was simultaneously implemented on the StepOnePlus™ Real-Time PCR System (ABI, Carlsbad, USA) with SYBR® Green Master Mix (Toyobo, Japan), and each sample was performed in triplicate. Thereafter, these data were calibrated using the $2^{-\triangle\triangle Ct}$ method.

2.4. Genomic Sequence Cloning and Structure Analysis

Genomic DNA was extracted from the tail using the Universal Genomic DNA Kit (CWBio, China). Specific primers (Table 2) were designed according to the predicted genomic sequences of *cyp19a1a* and *cyp19a1b* that were obtained from the blotched snakehead genome [34]. Then, PCR products were sequenced to verify the genomic sequences. The gene structure of *cyp19a1a* and *cyp19a1b* was determined by comparing the genomic sequence with the cDNA sequence. The putative promoters were predicted using Softberry (http://www.softberry.com/berry.phtml, accessed on 1 August 2022). The pu-

tative transcription factor binding sites (TFBS) were predicted using AnimalTFDB4.0 (http://bioinfo.life.hust.edu.cn/AnimalTFDB4/, accessed on 1 August 2022).

Table 2. Primers for genomic sequence cloning.

Primer Name	Sequence (5′–3′)	Length (bp)
Cyp19a1a-gDNA-F1	GCAACAAGGATTTTAGTAGGG	1490 bp
Cyp19a1a-gDNA-R1	GTGTGGCTCCAGGCGA	
Cyp19a1a-gDNA-F2	GTGTCAAGTCTCCCTCCCTAT	1379 bp
Cyp19a1a-gDNA-R2	CTTCTGTTCTACAAGGCTCTCTAT	
Cyp19a1a-gDNA-F3	GCCATAGAGAGCCTTGTAGAA	1147 bp
Cyp19a1a-gDNA-R3	CCGAATGGCTGGAAGTAAG	
Cyp19a1a-gDNA-F4	TAATTGGCTACTTCTCCCTAA	927 bp
Cyp19a1a-gDNA-R4	TGGTGATCTCAGTCTAACATACATA	
Cyp19a1b-gDNA-F1	GCAAAAGTGCAAGCCCAAC	1174 bp
Cyp19a1b-gDNA-R1	GAAGAAGCAGAATCGCAGTGA	
Cyp19a1b-gDNA-F2	TACTGGTGAGAGACACTTTATGAG	1388 bp
Cyp19a1b-gDNA-R2	CTGAGCAGATTGAGAGTGTCC	
Cyp19a1b-gDNA-F3	GGATGGAAGGAAGGGGT	1336 bp
Cyp19a1b-gDNA-R3	ATGAGACCAATGTTGAGAATG	
Cyp19a1b-gDNA-F4	CAACATCATTCTCAACATTGG	649 bp
Cyp19a1b-gDNA-R4	CTACTTGTGACTACACTTGCTTG	

2.5. Bisulfite Sequencing PCR (BSP)

Gonads and brain from the adult XX-F, XY-F, XY-M, and YY-M individuals (n = 3) and gonads at different developmental stages from XX-F and XY-M individuals (n = 3) were used for genomic DNA extraction and BSP. Approximately 600 ng of each genomic DNA sample was bisulfite-treated to obtain the methylated DNA using the EZ DNA Methylation-Gold™ Kit (Zymo Research, USA) according to the manufacturer's instructions. MethPrimer (http://www.urogene.org/cgi-bin/methprimer/methprimer.cgi, accessed on 1 August 2022) was used to predict CpG sites and design bisulfite-treated DNA-specific primers. Cyp19a1a-BSP-F1/R1 and Cyp19a1b-BSP-F1/R1 primer pairs were used for BSP amplification with methylated DNA as a template (Table 1). The amplified DNA fragments were cloned into pMD19-T vectors and transformed into *Escherichia coli* DH5α competent cells; positive clones were sequenced by the commercial company (Sangon Biotech, China). The total number of methylated cytosine was calculated as the average of the total number of methylated cytosine across the 10 sequenced positive clones from every fish (n = 3).

2.6. Statistical Analysis

Data were expressed as mean ± standard deviation (SD). Significant differences were subjected to one-way ANOVA followed by Dunnett's multiple comparisons post-test using SPSS Statistics 20. The correlation coefficient was calculated using Excel. Statistical significance was set at $p < 0.05$.

3. Results

3.1. Nucleotide and Amino Acid Sequences of cyp19a1a and cyp19a1b in C. maculata

The *cyp19a1a* cDNA sequence was 2054 bp long with an ORF (open reading frame) of 1554 bp, a 54 bp 5′UTR, and a 446 bp 3′UTR (GenBank Accession No. OP960399). Cyp19a1a encoded a putative protein of 517 amino acids, which included a P450 domain in 64~497 aa (Figure S1a). The *cyp19a1b* cDNA sequence was 1889 bp long with an ORF of 1464 bp, a 304 bp 5′UTR, and a 121 bp 3′UTR (GenBank Accession No. OP960400). Cyp19a1b encoded a putative protein of 487 amino acids, which included the signal peptides in 1~25 aa and a P450 domain in 32~473 aa (Figure S1c). The amino acid sequences of cyp19a1a and cyp19a1b showed 57.5% sequence identity with each other using DNAMAN (Figure S2).

The phylogenetic tree was constructed using 37 aromatase protein sequences from 26 species with the NJ algorithms. It indicated that the vertebrate aromatase proteins were

categorized as two clades, namely teleost aromatase and tetrapod aromatase, and the teleost aromatase was distinct from tetrapod aromatase that included the cartilaginous fish. Within the teleost clade, the single cyp19a1 sequences of basal teleosts were at the base of the subclade constituted by all duplicated cyp19a1 sequences from the crown teleosts that were clustered by cyp19a1a and cyp19a1b, which likely resulted from TWGD. The aromatase in *C. maculata* was clustered with the other teleost cyp19a1a and cyp19a1b, respectively. *C. maculata* cyp19a1a was placed closely with *M. albus* cyp19a1a, and *C. maculata* cyp19a1b also showed the highest identity with *M. albus* cyp19a1b (Figure 1). The result of the alignments among these aromatase protein sequences is shown in Figure S3.

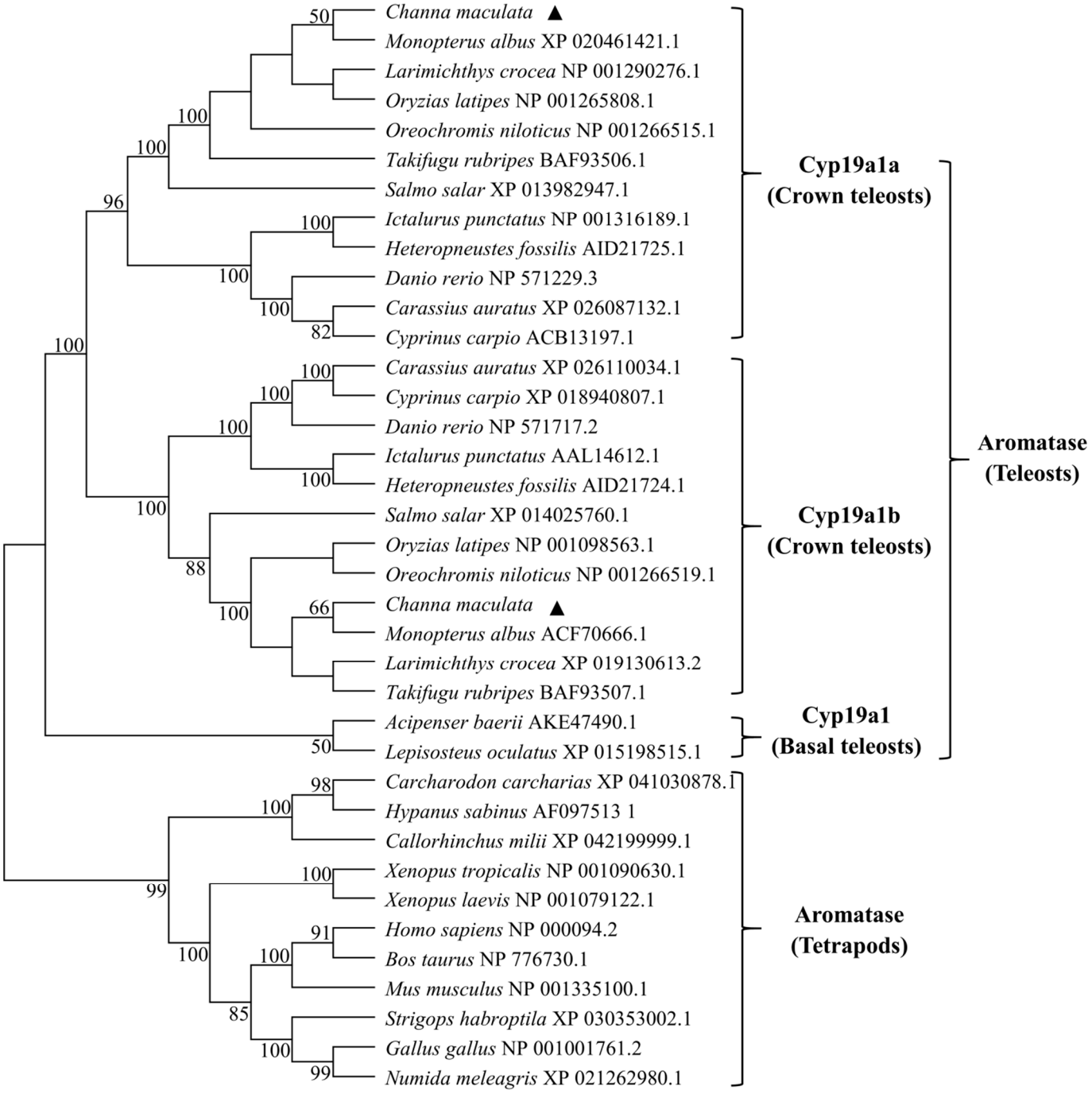

Figure 1. Phylogenetic analysis of vertebrate aromatase. The phylogenetic tree was constructed with the NJ method using Mega 6.0. The bootstrap values were calculated with 1000 replications, and the bar indicates the distance. The aromatase in *C. maculata* was marked with a triangle.

3.2. Gene Structure of cyp19a1a and cyp19a1b in C. maculata

The final assembled genomic sequences were 4540 bp and 3988 bp for *cyp19a1a* (GenBank Accession No. OP960401) and *cyp19a1b* (GenBank Accession No. OP960402), respectively, which contained a 5′-flanking region, the gene, and a 3′-flanking region (Figure 2).

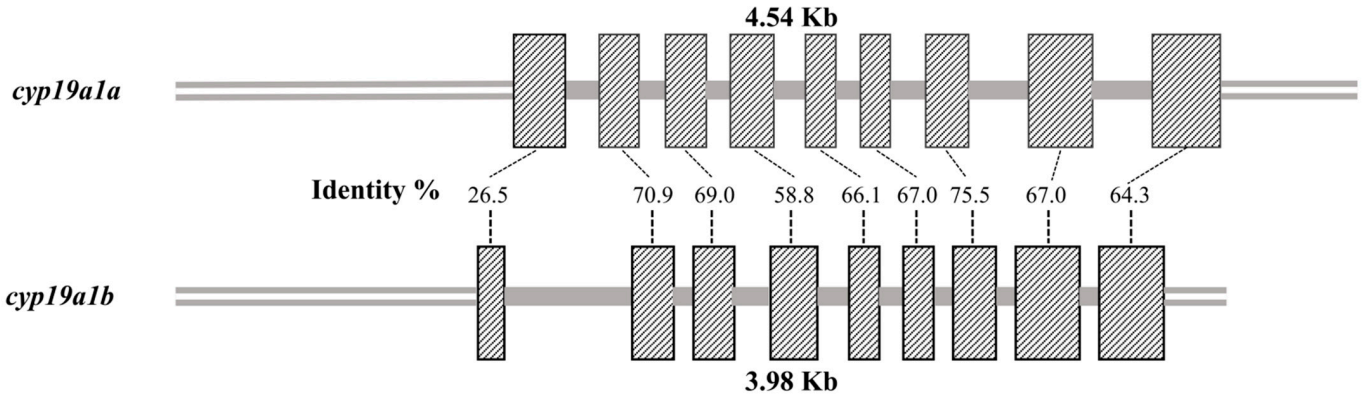

Figure 2. Gene structures of aromatase in *C. maculata*. The lengths of a 5′-flanking region, exon, intron, and 3′-flanking region are indicated in bp.

The aromatase genes were structurally conserved; both of them contained nine exons and eight relatively short introns, which were similar to other teleosts. Nine CpG sites were detected in the putative proximal promoter (−150 to +258 bp) in the 5′-flanking region of *cyp19a1a* (Figure S1b), and eight CpG sites were found in the distal *cyp19a1b* promoter at position −1009 to −691 bp (Figure S1d). The 5′-flanking region of aromatase contained a mass of putative TFBS, including the cAMP-responsive element (CRE), DM domain-containing transcription factors (DMRT), GATA, SRY-Box (SOX), FOXL, and TATA box (Figure S1), which are essential for the regulation of aromatase gene promoter activities.

3.3. Gene Expression of cyp19a1a and cyp19a1b in C. maculata

3.3.1. Gene Expression in Adult Tissues

Cyp19a1a showed sexual dimorphism in the expression patterns of gonads ($p < 0.01$), whose expression level in the female ovary (168.3 ± 8.2 folds change) was 10.8 times as much as that in the male testis (15.6 ± 0.7 folds change). *Cyp19a1a* had medium expression levels in the brain and the head kidney, and significant sexual dimorphism was noticed in the expression of the head kidney ($p < 0.01$), but not in the brain ($p > 0.05$). However, the expression levels in other tissues were extremely low, such as 0.23 ± 0.05 folds change in the female's gills (Figure 3a).

The expression level of *cyp19a1b* was exceedingly high in the brain, while there was no detectable difference in the male and female brain ($p > 0.05$). Nevertheless, the transcripts of *cyp19a1b* in the spleen ($p < 0.01$), intestine ($p < 0.05$), and muscle ($p < 0.05$) had obvious sexual dimorphism across sex, and it hardly expressed in other tissues (Figure 3b).

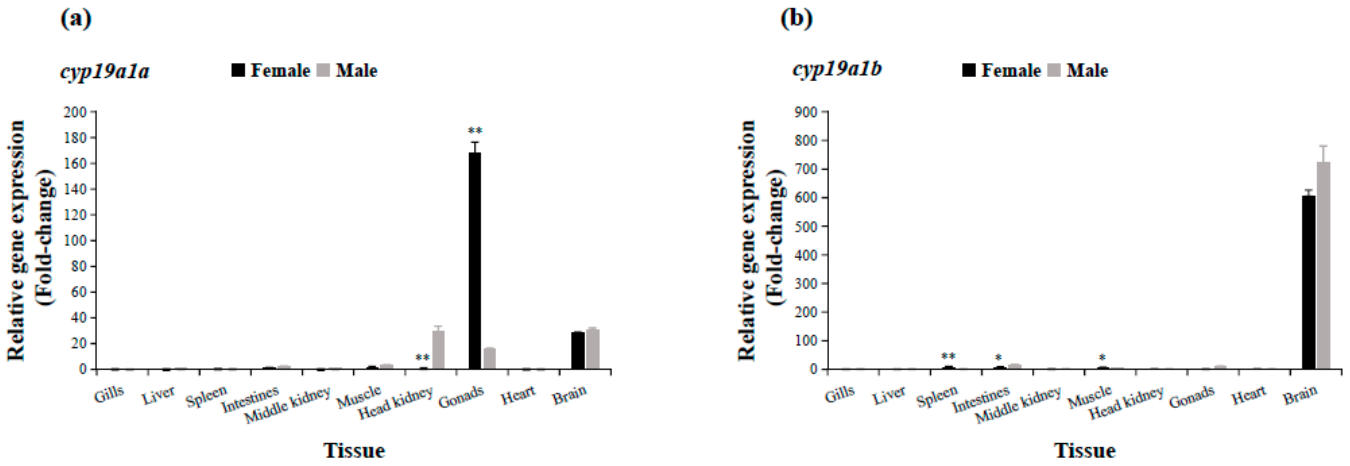

Figure 3. Relative gene expression of *cyp19a1a* (**a**) and *cyp19a1b* (**b**) in different tissues of adult female and male individuals (mean ± SD, n = 3). *β-actin* and *EF1α* are the internal control. * means there are significant differences between female and male individuals ($p < 0.05$). ** means there are extremely significant differences between female and male individuals ($p < 0.01$).

3.3.2. Gene Expression in Sex Reversal

Cyp19a1a demonstrated that the female-biased expression pattern in the ovary of XY-F (XY-F-O) resembled that in the ovary of XX-F (XX-F-O), and a low expression level in the testis of YY-M (YY-M-T) was similar to that in the testis of XY-M (XY-M-T). There were no significant sex variations in the expression levels of *cyp19a1b* between ovaries and testes ($p > 0.05$) (Figure 4a). Figure 4b indicated that *cyp19a1a* had relatively similar expression levels in the brain of XX-F (XX-F-B), the brain of XY-F (XY-F-B), the brain of XY-M (XY-M-B), and the brain of YY-M (YY-M-B). Similarly, the *cyp19a1b* transcripts were expressed with similar amounts in these four types of brain.

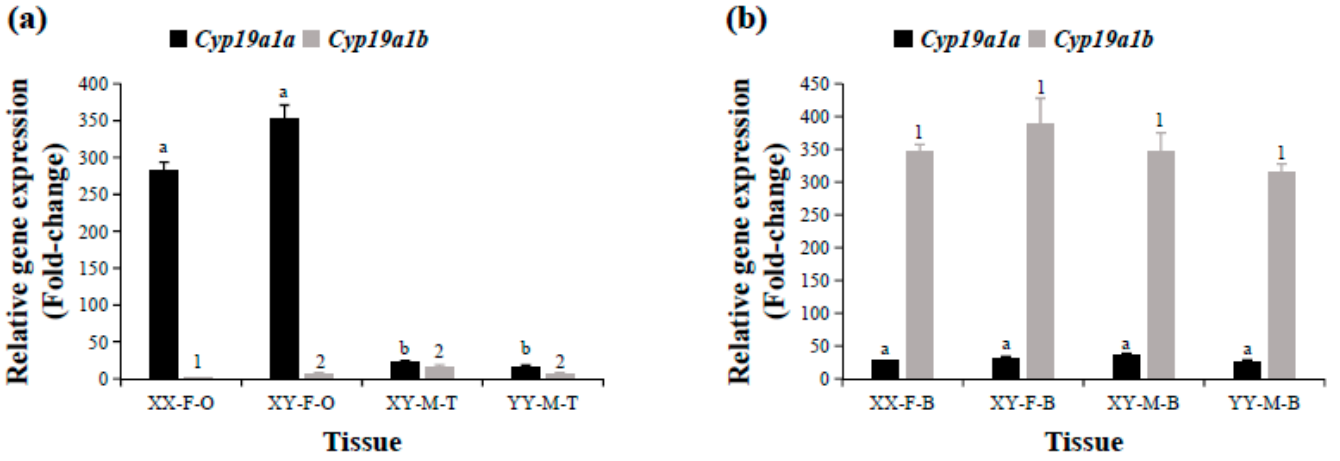

Figure 4. Relative gene expression of aromatase genes in the gonads (**a**) and brain (**b**) of adult XX-F, XY-F, XY-M, and YY-M individuals (mean ± SD, n = 3). Comparisons of *cyp19a1a* and *cyp19a1b* are indicated with superscript letters and numbers, respectively, and groups that bear different letters or numbers are significantly different ($p < 0.05$).

3.3.3. Gene Expression during the Gonadal Development Stage

Figure 5a indicated the expression levels of aromatase gene in the gonads of *C. maculata* during the different development stages. *Cyp19a1a* expression levels revealed significantly sexual dimorphism in the gonads, which were higher in the ovary than that in the testis at different developmental stages ($p < 0.05$). In the ovary, the transcripts of *cyp19a1a* increased from 30 dpf to 150 dpf, and reached a peak at 150 dpf ($p < 0.05$), then gradually declined

from 180 dpf. However, *cyp19a1a* always maintained a very low level at different testicular development stages. For *cyp19a1b*, its expression in the testis and the ovary had no obvious contrast at different developmental stages ($p > 0.05$), with relatively low levels.

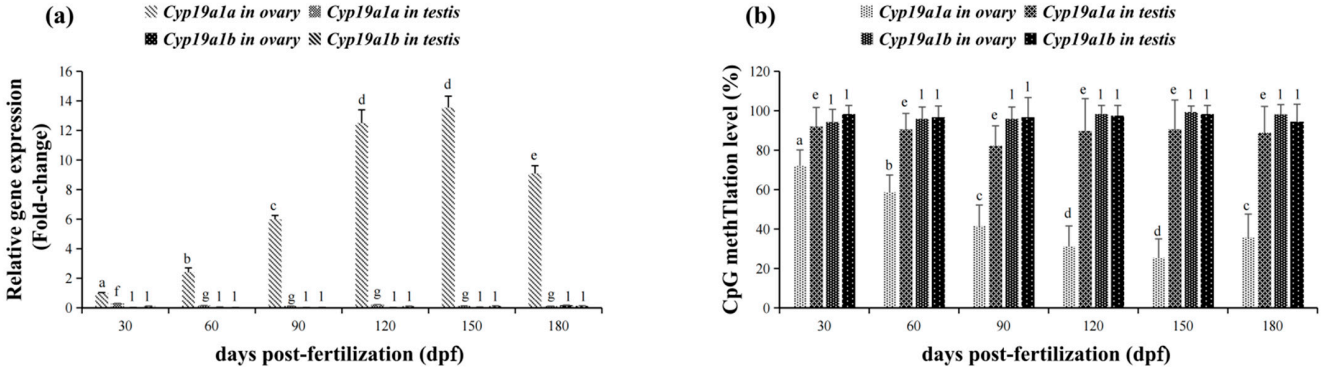

Figure 5. The expression profiles (**a**) and CpG methylation profiles (**b**) of the aromatase gene in the gonads of XX-F and XY-M individuals at different developmental stages (mean ± SD, n = 3). The superscript letters and numbers indicate comparisons between the *cyp19a1a* and *cyp19a1b* at different developmental stages, respectively. Groups that bear different letters or numbers are significantly different ($p < 0.05$).

3.4. CpG Methylation Levels of cyp19a1a and cyp19a1b in C. maculata

3.4.1. CpG Methylation Levels in Adult Gonads and Brain

The CpG methylation status of the aromatase gene promoter in *C. maculata* was analyzed using BSP technology. The CpG methylation levels of *cyp19a1a* promoter were 43.0 ± 10.1% in XX-F-O (Figure 6a) and 45.9 ± 10.2% in XY-F-O (Figure 6b), which were much lower than 97.0 ± 6.6% in XY-M-T (Figure 6c) and 91.9 ± 6.6% in YY-M-T (Figure 6d). Overall, there were striking variations in CpG methylation levels between the testis and the ovary. The correlation analysis indicated that the CpG methylation level of the *cyp19a1a* promoter was strongly negatively related to its mRNA expression in the gonad of *C. maculata*, and the correlation coefficient (R^2) was 0.9889 (Figure 8a). The CpG methylation levels of the *cyp19a1b* promoter were not significantly different between the testis and the ovary, which were 80.0 ± 12.3%, 74.2 ± 12.0%, 89.2 ± 4.4%, and 91.7 ± 9.0% in XX-F-O (Figure 6e), XY-F-O (Figure 6f), XY-M-T (Figure 6g), and YY-M-T (Figure 6h), respectively. Meanwhile, there was no obvious correlation between the CpG methylation level of the *cyp19a1a* promoter and its expression in the gonad ($R^2 = 0.2115$) (Figure 8b).

At the same time, the CpG methylation levels of *cyp19a1a* and *cyp19a1b* in the four types of adult brain were also analyzed. Figure 7 revealed that *cyp19a1a* and *cyp19a1b* were highly methylated in the brain, no matter what type. The CpG methylation levels of *cyp19a1a* were slightly lower than that of *cyp19a1b*, which were 70.4~78.5%, and there were no significant differences among them. *Cyp19a1b* showed hypermethylation with 98.3 ± 4.4%, 94.2 ± 11.4%, 93.3 ± 16.3%, and 94.2 ± 10.4% in XX-F-B (Figure 7e), XY-F-B (Figure 7f), XY-M-B (Figure 7g), and YY-M-B (Figure 7h), respectively, and three loci (1, 5, 8) were even 100% methylated in the brain.

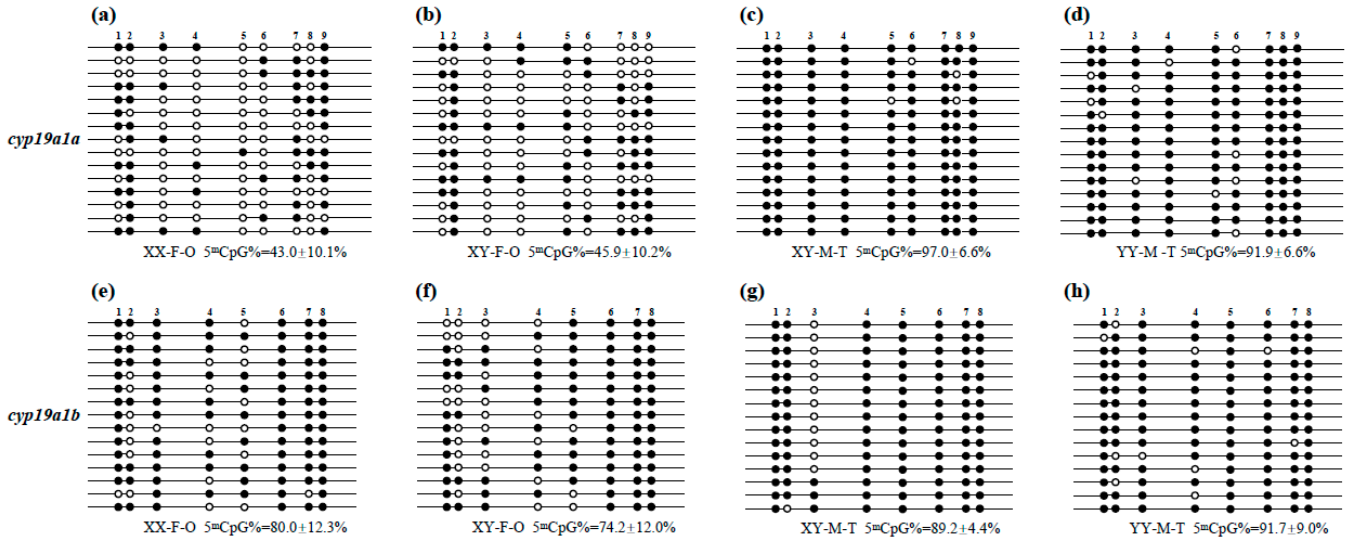

Figure 6. The CpG methylation profiles of *cyp19a1a* (**a**–**d**) and *cyp19a1b* (**e**–**h**) in the gonads of adult XX-F, XY-F, XY-M, and YY-M individuals (mean ± SD, n = 3). The hollow circles mean the unmethylated CpG loci, and the solid circles mean the methylated CpG loci.

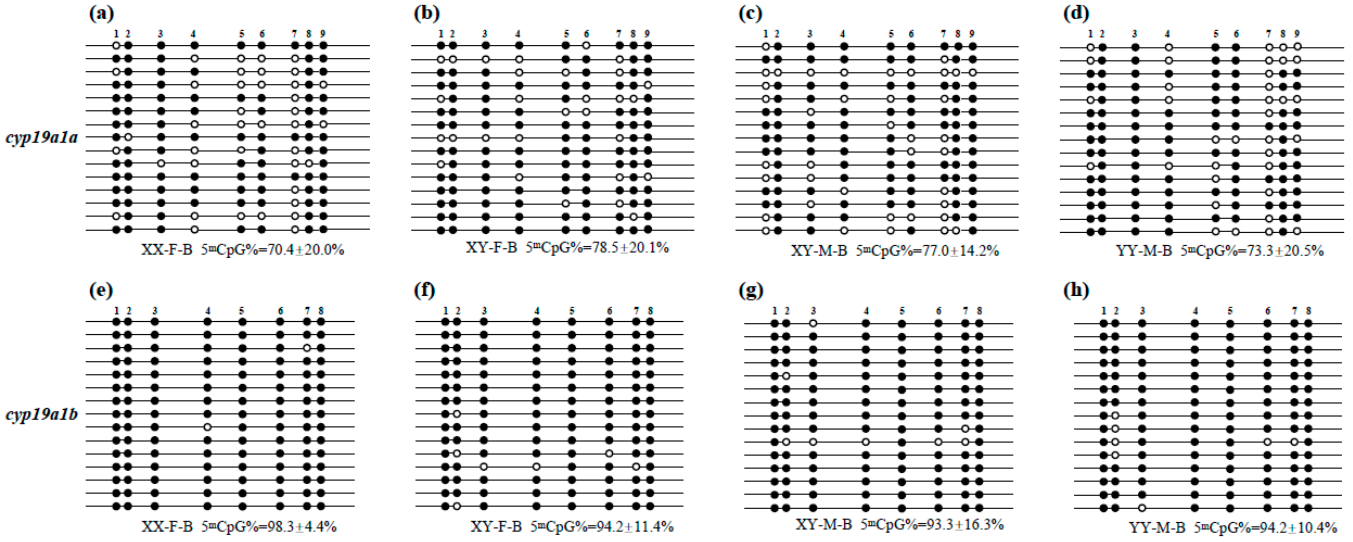

Figure 7. The CpG methylation profiles of *cyp19a1a* (**a**–**d**) and *cyp19a1b* (**e**–**h**) in the brains of adult XX-F, XY-F, XY-M, and YY-M individuals (mean ± SD, n = 3). The hollow circles mean the unmethylated CpG loci, and the solid circles mean the methylated CpG loci.

The correlation analysis also demonstrated that there were no obvious correlations between CpG methylation levels and the mRNA expression of *cyp19a1a* (Figure 8c) and *cyp19a1b* (Figure 8d) in the brain of *C. maculata*, and R^2 were 0.4257 and 0.0018, respectively.

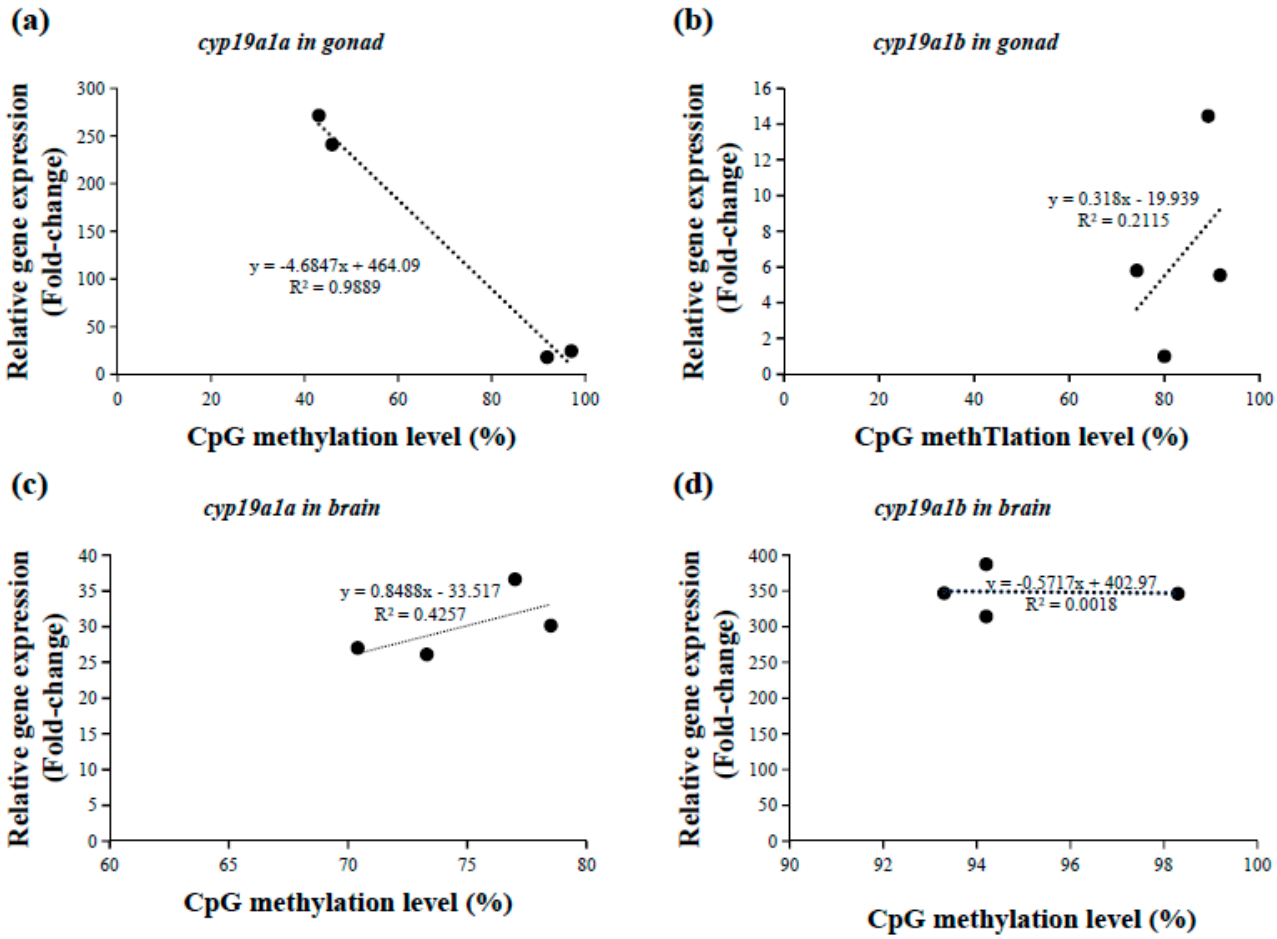

Figure 8. The relationship between the CpG methylation levels and the expression levels of the aromatase gene in gonads (**a**,**b**) and the brain (**c**,**d**).

3.4.2. CpG Methylation Levels during the Gonadal Development Stage

As shown in Figure 5b, there were marked distinctions in the CpG methylation levels of *cyp19a1a* promoter between the ovary and the testis during gonadal development stage ($p < 0.05$). In the ovary, the CpG methylation levels of *cyp19a1a* promoter declined from 30 dpf to 150 dpf, with the lowest levels at 150 dpf (25.2 ± 9.8%), and then gradually increased from 180 dpf. Nevertheless, the methylation levels of *cyp19a1a* promoter in the male testis were relatively high at different developmental stages, with no sharp distinction. The CpG methylation levels of *cyp19a1b* promoter displayed no significant differences between the testis and the ovary at different developmental stages ($p > 0.05$), and the average methylation levels were at least 90% in the gonads, regardless of sex.

The correlation analysis revealed that the gene expression levels of *cyp19a1a* in the ovary were negatively correlated with its CpG methylation levels at developmental stages ($R^2 = 0.9197$) (Figure S4a), but there was no obvious correlation between the gene expression levels of *cyp19a1a* and its CpG methylation levels at testicular development stages ($R^2 = 0.2567$) (Figure S4c). For *cyp19a1b*, its expression was not related to the methylation levels during gonadal development, whether in the ovary ($R^2 = 0.151$) (Figure S2b) or the testis ($R^2 = 0.0004$) (Figure S4d).

4. Discussion

In this study, two aromatase genes, *cyp19a1a* and *cyp19a1b*, were characterized from *C. maculata* that is susceptible to hormone-induced sex reversal, in accordance with two structurally and functionally different *cyp19a* isoforms that have been found in most teleosts [17,19,36]. The phylogenetic analysis indicated that cyp19a1a and cyp19a1b in

C. maculata shared high identities with the corresponding homologues in other crown teleosts, respectively, than between themselves, suggesting a coevolutionary ancestry of the respective isoforms that likely resulted from TWGD [37]. *Cyp19a1a* and *cyp19a1b* in *C. maculata* included nine exons and eight introns, which were similar to other vertebrate aromatases, such as *H. sapien* [15], *X. laevis* [14], *Lateolabrax maculatus* [38], *P. pulcher* [19], etc. Interestingly, the similarities of each exon between *cyp19a1a* and *cyp19a1b* in *C. maculata* were about 58.8~70.9%, except for the first exon, which was only 26.5%. It may be due to adapt to the TWGD that the first exon of *cyp19a1b* was obviously shorter than that of *cyp19a1a* in *C. maculata*, which leads to this result. Of course, this needs to be further studied.

In most teleosts, *cyp19a1a* is mainly expressed in the gonad [10,12] and *cyp19a1b* in the brain [18,19]. *C. maculata cyp19a1a* had a female-biased expression pattern in the gonad, and its expression in the ovary was much higher than that in the testis. Similar results were demonstrated in *H. fossilis* [36], *Oncorhynchus mykiss* [39], *Schizothorax prenanti* [40], and so on. Even though the particularly dominant expression levels of *cyp19a1a* were detected in the ovary, it also expressed in other tissues, including the testis at low levels. Nevertheless, the *cyp19a1a* genes in *Melanotaenia fluviatilis, Odontesthes bonariensis*, *O. niloticus*, and *Fundulus heteroclitus* have been found to be exclusively expressed in the ovary [37]. This pattern of specific and restricted expression of *cyp19a1a* in the ovary was consistent with the well-known high estrogenic activity of the ovary and the role of estrogen in ovarian development and growth [12]. The expression level of *cyp19a1b* transcripts in *C. maculata* were significantly higher in the brain compared with other tested tissues, and there was no detectable difference between sexes, which was in accordance with *P. pulcher* [18]. There are enormous variations in the expression patterns of *cyp19a1b* in the brain of teleosts. Male-biased *cyp19a1b* activity has been reported in *C. carpio* [41], *M. fluviatilis* [37], etc. Conversely, female-biased *cyp19a1b* activity has been found in *D. rerio* and *O. latipes* [18]. These remarkable differences in expression patterns of the *cyp19a1b* across species and between sexes are likely to reflect the multitudinous behavioral and reproductive variations observed in teleosts [37].

Environmental factors, such as exogenous estrogen, endocrine-disrupting chemicals, and temperature, could induce sex reversal in teleosts. In our previous study, feminization was induced in normal XY males by estrogen, and the gonad differentiated into the ovary [31]. The molecular mechanism involved in sex reversal has been the focus of increasing attention; the conserved *cyp19a1* gene usually participates in the process of sex reversal. Furthermore, epigenetic modification of *cyp19a1* promoter is closely related to the regulation of *cyp19a1a* expression in the switching of sex pathways [21,22]. Therefore, the expression and CpG methylation analyses of aromatase genes were conducted on the gonad and brain from the adult XX-F, XY-F, XY-M, and YY-M blotched snakehead. The *cyp19a1a* expression pattern in the XY-F ovary was similar to that in the XX-F ovary, with relatively high expression levels, which were far higher than those in XY-M and YY-M testes. On the contrary, CpG methylation levels of *cyp19a1a* promoter were lower in the ovaries of XX-F and XY-F compared with the testes of XY-M and YY-M. There was an inverse correlation between *cyp19a1a* expression and CpG methylation levels of *cyp19a1a* promoter in the gonad. Similar results were also observed in the sex reversal of genetic males to phenotypic females in *A. schlegelii* [25], and the sex reversal of genetic females to phenotypic males in *D. labrax* [26], *M. albus* [23], *C. semilaevis* [27], *O. niloticus* [29], *P. olivaceus* [28], and *E. coioides* [24], wherein DNA methylation is inversely responsible for *cyp19a1a* expression. The CpG methylation levels of *cyp19a1b* promoter were similar to *cyp19a1b* expression in gonads, and there were no significant sexual variations. Similarly, the CpG methylation levels of *cyp19a1a* and *cyp19a1b* promoters in the brain had no differences within sexes, with 70.4~78.5% in *cyp19a1a* promoter and 93.3~98.3% in *cyp19a1b* promoter, respectively. These findings suggest that increased *cyp19a1a* expression is associated with the initiation of male-to-female sex reversal in *C. maculata*, and DNA methylation may represent a crucial factor in maintaining the sexual dimorphism of *cyp19a1a* expression in gonads. However, the function of *cyp19a1b* in *C. maculata* needs further research.

We have conducted histological observations of the ovary during different phases of development in *C. maculata* (unpublished data); referring to the reports of *C. argus* [42], the oocyte development in *C. maculata* were divided into six phases: oogonia phase, monolayer follicular phase, vitellogenesis phase, engorged vitelline phase, mature oocyte phase, and degraded oocyte phase. In addition, the maturation of ovaries goes through six stages (I–VI) according to oocyte development. The ovarian estrogen level increases up to the completion of vitellogenesis and decreases in the post-vitellogenic ovary [43]. In this study, *cyp19a1a* activity was markedly increased from 30 dpf to 150 dpf, and reached the maximum value at 150 dpf. Histology indicated that 150 dpf ovary was in stage III; at this time, the oocyte was in the mid-vitellogenic phase. These results suggested that *C. maculata* cyp19a1a played an important role in ovarian maturation, which caused greater conversion of androgen to estrogen, thus leading to an increase in the concentration of E2 in the plasma. Furthermore, *cyp19a1a* activity began to decrease at 180 dpf ovary, whose oocyte was in the late vitellogenic phase. The variation of *cyp19a1a* expression in *C. maculata* was basically consistent with the variation trend of estrogen concentration that we have reported that estrogen level peaked at 135 days post hatching (dph) and began to decline at 165 dph [44]. Similar findings were reported in *I. punctatus* [45], *O. niloticus* [46], *M. albus* [23], *S. prenanti* [40], and so on. These findings reaffirmed that cyp19a1a exhibited an obvious correlation with the function of estrogen during ovarian development in *C. maculata*. Likewise, there is no consistent sex bias for *cyp19a1b* expression during gonadal development.

As expected, the overall methylation levels of *cyp19a1a* promoter were inversely correlated with *cyp19a1a* expression in *C. maculata* during the ovarian development stage. Similarly, the methylation levels had an inverse relationship with *cyp19a1a* expression during different ovarian follicle developmental stages in *D. rerio* [47]. The DNA methylation status of ovarian *cyp19a1a* promoter was associated with the sexual phase of *A. schlegelii* [25]. The significantly demethylated phenomenon of *cyp19a* promoter was detected at the early ovarian differentiation stage in *P. olivaceus* [28]. Taken together, the results indicated that epigenetic modification plays a crucial role in maintaining the sexually dimorphic expression of *cyp19a1a*, ovarian differentiation, and oogenesis in teleosts.

5. Conclusions

In conclusion, two aromatase genes were isolated from *C. maculata*, ovarian aromatase *cyp19a1a* and brain aromatase *cyp19a1b.* According to the structure, sequence similarity, and phylogenetic analysis, cyp19a1a and cyp19a1b were highly conserved from a coevolutionary ancestry of the respective isoforms. *Cyp19a1a* exhibited strong female-biased expression patterns in the ovary, and *cyp19a1b* dominantly expressed in the brain with no sex bias. Cyp19a1a played an important role in the hormone-induced sex reversal of *C. maculata*; its expression pattern in the XY-F ovary was similar to that in the XX-F ovary, with a relatively high expression level, which was far higher than that in the XY-M and YY-M testes. Meanwhile, CpG methylation levels of *cyp19a1a* promoter were lower in the ovaries of XX-F and XY-F compared with the testes of XY-M and YY-M. A significant negative correlation between the CpG methylation level and *cyp19a1a* expression was elucidated. During different ovarian developmental stages, the strongly female-biased *cyp19a1a* expression was closely related to ovarian differentiation and maturation; furthermore, the overall methylation levels of *cyp19a1a* promoter were inversely correlated with *cyp19a1a* expression. There were no detectable sexually dimorphic differences in the expression levels of *cyp19a1b* transcripts and the CpG methylation levels of *cyp19a1b* promoter in the brain and gonad of *C. maculata*; thus, the function of *cyp19a1b* in *C. maculata* needs further research. Our research illustrates that cyp19a1a is closely related to estrogen production, ovary differentiation/maintenance, and sex reversal in *C. maculata*, and epigenetic modification plays a crucial role in maintaining the sexual dimorphic expression of *cyp19a1a*, ovarian differentiation, and oogenesis.

Supplementary Materials: The following supporting information can be downloaded at: https://www.mdpi.com/article/10.3390/fishes8030129/s1.

Author Contributions: Conceptualization, S.H., M.O.; data curation, S.H., Y.W.; formal analysis, S.H., X.Z. (Xiaotian Zhang), H.L.; funding acquisition, K.C., M.O.; investigation, S.H., Y.W., X.Z. (Xiaotian Zhang), Q.L.; project administration, J.Z., M.O.; visualization, F.W., K.L., X.Z. (Xincheng Zhang), S.F.; writing—original draft, S.H., Y.W.; writing-review and editing, J.Z., K.C., M.O. All authors have read and agreed to the published version of the manuscript.

Funding: This work was supported by the Basic and Applied Basic Research Foundation of Guangdong Province (2021A1515012075), the Science and Technology Program of Guangzhou (202201010120), the National Natural Science Foundation of China (31902351), the Central Public-interest Scientific Institution Basal Research Fund, CAFS (2020TD34), and the China Agriculture Research System of MOF and MARA (CARS-46).

Institutional Review Board Statement: All fish experiments in the present study were approved by the Pearl River Fisheries Research Institute and the Chinese Academy of Fishery Sciences, and they were performed following the institutional ethical guidelines for experimental animals.

Informed Consent Statement: Not applicable.

Data Availability Statement: The data presented in this study are available in the article. Further information is available upon request from the corresponding author.

Conflicts of Interest: The authors declare no conflict of interest.

References

1. Mei, J.; Gui, J.F. Genetic basis and biotechnological manipulation of sexual dimorphism and sex determination in fish. *Sci. China Life. Sci.* **2015**, *58*, 124–136. [CrossRef] [PubMed]
2. Berta, P.; Hawkins, J.R.; Sinclair, A.H.; Taylor, A.; Griffiths, B.L.; Goodfellow, P.N.; Fellous, M. Genetic evidence equating *SRY* and the testis-determining factor. *Nature* **1990**, *348*, 448–450. [CrossRef] [PubMed]
3. Natri, H.M.; Merilä, J.; Shikano, T. The evolution of sex determination associated with a chromosomal inversion. *Nat. Commun.* **2019**, *10*, 145. [CrossRef] [PubMed]
4. Li, X.Y.; Mei, J.; Ge, C.T.; Liu, X.L.; Gui, J.F. Sex determination mechanisms and sex control approaches in aquaculture animals. *Sci. China Life Sci.* **2022**, *65*, 1091–1122. [CrossRef]
5. Piferrer, F.; Ribas, L.; Díaz, N. Genomic approaches to study genetic and environmental influences on fish sex determination and differentiation. *Mar. Biotechnol.* **2012**, *14*, 591–604. [CrossRef]
6. Li, M.; Sun, L.; Wang, D. Roles of estrogens in fish sexual plasticity and sex differentiation. *Gen. Comp. Endocrinol.* **2019**, *277*, 9–16. [CrossRef]
7. Herpin, A.; Schartl, M. Plasticity of gene-regulatory networks controlling sex determination: Of masters, slaves, usual suspects, newcomers, and usurpators. *EMBO Rep.* **2015**, *16*, 1260–1274. [CrossRef]
8. Crespo, B.; Gómez, A.; Mazón, M.J.; Carrillo, M.; Zanuy, S. Isolation and characterization of Ff1 and Gsdf family genes in European sea bass and identification of early gonadal markers of precocious puberty in males. *Gen. Comp. Endocrinol.* **2013**, *191*, 155–167. [CrossRef]
9. Capel, B. Vertebrate sex determination: Evolutionary plasticity of a fundamental switch. *Nat. Rev. Genet.* **2017**, *18*, 675–689. [CrossRef]
10. Wu, K.; Song, W.; Zhang, Z.W.; Ge, W. Disruption of *dmrt1* rescues the all-male phenotype of *cyp19a1a* mutant in zebrafish—A novel insight into the roles of aromatase/estrogens in gonadal differentiation and early folliculogenesis. *Development* **2020**, *147*, 182758. [CrossRef]
11. Dai, S.; Qi, S.; Wei, X.; Liu, X.; Li, Y.; Zhou, X.; Xiao, H.; Lu, B.; Wang, D.; Li, M. Germline sexual fate is determined by the antagonistic action of *dmrt1* and *foxl3/foxl2* in tilapia. *Development* **2021**, *148*, 199380. [CrossRef] [PubMed]
12. Guiguen, Y.; Fostier, A.; Piferrer, F.; Chang, C.F. Ovarian aromatase and estrogens: A pivotal role for gonadal sex differentiation and sex change in fish. *Gen. Comp. Endocrinol.* **2010**, *165*, 352–366. [CrossRef] [PubMed]
13. Coumailleau, P.; Pellegrini, E.; Adrio, F.; Diotel, N.; Cano-Nicolau, J.; Nasri, A.; Vaillant, C.; Kah, O. Aromatase, estrogen receptors and brain development in fish and amphibians. *BBA Gene. Regul. Mech.* **2015**, *1849*, 152–162. [CrossRef] [PubMed]
14. Miyashita, K.; Shimizu, N.; Osanai, S.; Miyata, S. Sequence analysis and expression of the P450 aromatase and estrogen receptor genes in the *Xenopus* ovary. *J. Steroid. Biochem.* **2000**, *75*, 101–107. [CrossRef]
15. Bulun, S.E.; Sebastian, S.; Takayama, K.; Suzuki, T.; Sasano, H.; Shozu, M. The human *CYP19* (aromatase P450) gene: Update on physiologic roles and genomic organization of promoters. *J. Steroid Biochem.* **2003**, *86*, 219–224. [CrossRef] [PubMed]
16. Golovine, K.; Schwerin, M.; Vanselow, J. Three different promoters control expression of the aromatase cytochrome P450 gene (*Cyp19*) in mouse gonads and brain. *Biol. Reprod.* **2003**, *68*, 978–984. [CrossRef] [PubMed]

17. Lin, C.J.; Maugars, G.; Lafont, A.G.; Jeng, S.R.; Wu, G.C.; Dufour, S.; Chang, C.F. Basal teleosts provide new insights into the evolutionary history of teleost-duplicated aromatase. *Gen. Comp. Endocrinol.* **2020**, *291*, 113395. [CrossRef] [PubMed]
18. Diotel, N.; Page, Y.L.; Mouriec, K.; Tong, S.-K.; Pellegrini, E.; Vaillant, C.; Anglade, I.; Brion, F.; Pakdel, F.; Chung, B.; et al. Aromatase in the brain of teleost fish: Expression, regulation and putative functions. *Front. Neuroendocr.* **2010**, *31*, 172–192. [CrossRef]
19. Driscoll, R.M.; Faber-Hammond, J.J.; O'Rourke, C.F.; Hurd, P.L.; Renn, S.C. Epigenetic regulation of gonadal and brain aromatase expression in a cichlid fish with environmental sex determination. *Gen. Comp. Endocrinol.* **2020**, *296*, 113538. [CrossRef]
20. Wang, H.; Piferrer, F.; Chen, S.; Shen, Z. *Sex Control in Aquaculture*; John Wiley&Sons Ltd.: Oxford, UK, 2018.
21. Todd, E.V.; Ortega-Recalde, O.; Liu, H.; Lamm, M.S.; Rutherford, K.M.; Cross, H.; Black, M.A.; Kardailsky, O.; Graves, J.A.M.; Hore, T.A.; et al. Stress, novel sex genes and epigenetic reprogramming orchestrate socially-controlled sex change. *Sci. Adv.* **2018**, *5*, 7006. [CrossRef]
22. Ortega-Recalde, O.; Goikoetxea, A.; Hore, T.A.; Todd, E.V.; Gemmell, N.J. The genetics and epigenetics of sex change in fish. *Annu. Rev. Anim. Biosci.* **2020**, *8*, 47–69. [CrossRef] [PubMed]
23. Zhang, Y.; Zhang, S.; Liu, Z.; Zhang, L.; Zhang, W. Epigenetic modifications during sex change repress gonadotropin stimulation of *cyp19a1a* in a teleost ricefield eel (*Monopterus albus*). *Endocrinology* **2013**, *154*, 2881–2890. [CrossRef]
24. Guo, C.Y.; Tseng, P.W.; Hwang, J.S.; Wu, G.C.; Chang, C.F. Potential role of DNA methylation of *cyp19a1a* promoter during sex change in protogynous orange-spotted grouper, *Epinephelus coioides*. *Gen. Comp. Endocrinol.* **2021**, *311*, 113840. [CrossRef] [PubMed]
25. Wu, G.C.; Li, H.W.; Huang, C.H.; Lin, H.J.; Lin, C.J.; Chang, C.F. The testis is a primary factor that contributes to epigenetic modifications in the ovaries of the protandrous black porgy, *Acanthopagrus schlegelii*. *Biol. Reprod.* **2016**, *94*, 132. [CrossRef] [PubMed]
26. Navarro-Martín, L.; Viñas, J.; Ribas, L.; Díaz, N.; Gutiérrez, A.; Di Croce, L.; Piferrer, F. DNA methylation of the gonadal aromatase (*cyp19a*) promoter is involved in temperature-dependent sex ratio shifts in the European sea bass. *PLoS Genet.* **2011**, *7*, e1002447. [CrossRef]
27. Shao, C.; Li, Q.; Chen, S.; Zhang, P.; Lian, J.; Hu, Q.; Sun, B.; Jin, L.; Liu, S.; Wang, Z.; et al. Epigenetic modification and inheritance in sexual reversal of fish. *Genome Res.* **2014**, *24*, 604–615. [CrossRef] [PubMed]
28. Fan, Z.; Zou, Y.; Jiao, S.; Tan, X.; Wu, Z.; Liang, D.; Zhang, P.; You, F. Significant association of *cyp19a* promoter methylation with environmental factors and gonadal differentiation in olive flounder *Paralichthys olivaceus*. *Comp. Biochem. Physiol. A* **2017**, *208*, 70–79. [CrossRef]
29. Wang, Y.Y.; Sun, L.X.; Zhu, J.J.; Zhao, Y.; Wang, H.; Liu, H.J.; Ji, X.S. Epigenetic control of *cyp19a1a* expression is critical for high temperature induced Nile tilapia masculinization. *J. Therm. Biol.* **2017**, *69*, 76–84. [CrossRef]
30. Bureau of Fisheries; Ministry of Agriculture. *China Fishery Statistics Yearbook 2022*; Agriculture Press: Beijing, China, 2022.
31. Ou, M.; Chen, K.; Gao, D.; Wu, Y.; Chen, Z.; Luo, Q.; Liu, H.; Zhao, J. Comparative transcriptome analysis on four types of gonadal tissues of blotched snakehead (*Channa maculata*). *Comp. Biochem. Physiol. D* **2020**, *35*, 100708. [CrossRef]
32. Zhao, J.; Ou, M.; Wang, Y.; Liu, H.; Luo, Q.; Zhu, X.; Chen, B.; Chen, K. Breeding of YY super-male of blotched snakehead (*Channa maculata*) and production of all-male hybrid (*Channa argus* ♀× *C. maculata* ♂). *Aquaculture* **2021**, *538*, 736450. [CrossRef]
33. Ou, M.; Chen, K.; Gao, D.; Wu, Y.; Luo, Q.; Liu, H.; Zhao, J. Characterization, expression and CpG methylation analysis of *Dmrt1* and its response to steroid hormone in blotched snakehead (*Channa maculata*). *Comp. Biochem. Physiol. B* **2022**, *257*, 110672. [CrossRef] [PubMed]
34. Ou, M.; Huang, R.; Yang, C.; Gui, B.; Luo, Q.; Zhao, J.; Li, Y.; Liao, L.; Zhu, Z.; Wang, Y.; et al. Chromosome-level genome assemblies of Channa argus and Channa maculata and comparative analysis of their temperature adaptability. *Gigascience* **2021**, *10*, giab070. [CrossRef] [PubMed]
35. Mao, H.; Chen, K.; Zhu, X.; Luo, Q.; Zhao, J.; Li, W.; Wu, X.; Xu, H. Identification of suitable reference genes for quantitative real-time PCR normalization in blotched snakehead *Channa maculata*. *J. Fish Biol.* **2017**, *90*, 2312–2322. [CrossRef] [PubMed]
36. Chaube, R.; Rawat, A.; Joy, K.P. Molecular cloning and characterization of brain and ovarian cytochrome P450 aromatase genes in the catfish *Heteropneustes fossilis*: Sex, tissue and seasonal variation in, and effects of gonadotropin on gene expression. *Gen. Comp. Endocrinol.* **2015**, *221*, 120–133. [CrossRef] [PubMed]
37. Shanthanagouda, A.H.; Patil, J.G.; Nugegoda, D. Ontogenic and sexually dimorphic expression of *cyp19* isoforms in the rainbowfish, *Melanotaenia fluviatilis* (Castelnau 1878). *Comp. Biochem. Physiol. A* **2012**, *161*, 250–258. [CrossRef] [PubMed]
38. Chen, X.; He, Y.; Wang, Z.; Li, J. Expression and DNA methylation analysis of *cyp19a1a* in Chinese sea perch *Lateolabrax maculatus*. *Comp. Biochem. Phys. B* **2018**, *226*, 85–90. [CrossRef]
39. Delalande, C.; Goupil, A.S.; Lareyre, J.J.; Le Gac, F. Differential expression patterns of three aromatase genes and of four estrogen receptors genes in the testes of trout (*Oncorhynchus mykiss*). *Mol. Reprod. Dev.* **2015**, *82*, 694–708. [CrossRef]
40. Yan, T.; Cai, Y.; He, J.; Zhang, Q.; Wang, X.; Zhang, S.; He, L.; He, Z. Characterization and expression profiles of *cyp19a1a* in the schizothoracine fish *Schizothorax prenanti*. *Tissue Cell* **2019**, *58*, 70–75. [CrossRef]
41. Barney, M.L.; Patil, J.G.; Gunasekera, R.M.; Carter, C.G. Distinct cytochrome P450 aromatase isoforms in the common carp (*Cyprinus carpio*): Sexual dimorphism and onset of ontogenic expression. *Gen. Comp. Endocr.* **2008**, *156*, 499–508. [CrossRef]
42. Yue, Z.; Gao, S.; Deng, F.; Xu, H.; Liu, Z. A histological study on the ovary development of *Channa argus*. *J. Wuhan Univ.* **1996**, *42*, 225–232. (In Chinese) [CrossRef]

43. Mishra, A.; Joy, K.P. Effects of gonadotropin in vivo and 2-hydroxyestradiol-17β in vitro on follicular steroid hormone profile associated with oocyte maturation in the catfish *Heteropneustes fossilis*. *J. Endocrinol.* **2006**, *189*, 341–353. [CrossRef]
44. Wu, Y.; Ou, M.; Gao, D.; Chen, K.; Luo, Q.; Liu, H.; Zhao, J. Molecular cloning, expression and response of *Foxl2* gene indued by sex steroid hormones in blotched snakehead (*Channa maculata*). *J. Dalian Ocean Uni.* **2022**, *37*, 49–50. (In Chinese) [CrossRef]
45. Kumar, R.S.; Ijiri, S.; Trant, J.M. Changes in the expression of genes encoding steroidogenic enzymes in the channel catfish (*Ictalurus punctatus*) ovary throughout a reproductive cycle. *Biol. Reprod.* **2000**, *63*, 1676–1682. [CrossRef]
46. Harvey, S.C.; Kwon, J.Y.; Penman, D.J. Physical mapping of the brain and ovarian aromatase genes in the Nile Tilapia, *Oreochromis niloticus*, by fluorescence in situ hybridization. *Anim. Genet.* **2003**, *34*, 62–64. [CrossRef] [PubMed]
47. Bai, J.; Gong, W.; Wang, C.; Gao, Y.; Hong, W.; Chen, S.X. Dynamic methylation pattern of *cyp19a1a* core promoter during zebrafish ovarian folliculogenesis. *Fish Physiol. Biochem.* **2016**, *42*, 947–954. [CrossRef] [PubMed]